ACS Catalysis

Research Article

pubs.acs.org/acscatalysis

Highly Efficient and Selective Hydrogenation of Aldehydes: A Well-Defined Fe(II) Catalyst Exhibits Noble-Metal Activity

Nikolaus Gorgas,[†] Berthold Stöger,[‡] Luis F. Veiros,[§] and Karl Kirchner*[,†]

[†]Institute of Applied Synthetic Chemistry and [‡]Institute of Chemical Technologies and Analytics, Vienna University of Technology, Getreidemarkt 9, A-1060 Vienna, Austria

[§]Centro de Química Estrutural, Instituto Superior Técnico, Universidade de Lisboa, Av. Rovisco Pais No. 1, 1049-001 Lisboa, Portugal

Supporting Information

ABSTRACT: The synthesis and application of [Fe(PNP^{Me}-*i*Pr)(CO)(H)(Br)] and [Fe(PNP^{Me}-*i*Pr)(H)$_2$(CO)] as catalysts for the homogeneous hydrogenation of aldehydes is described. These systems were found to be among the most efficient catalysts for this process reported to date and constitute rare examples of a catalytic process which allows selective reduction of aldehydes in the presence of ketones and other reducible functionalities. In some cases, TONs and TOFs of up to 80000 and 20000 h^{-1}, respectively, were reached. On the basis of stoichiometric experiments and computational studies, a mechanism which proceeds via a *trans*-dihydride intermediate is proposed. The structure of the hydride complexes was also confirmed by X-ray crystallography.

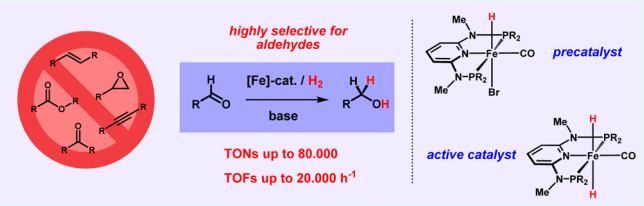

KEYWORDS: *aldehyde hydrogenation, iron pincer complexes, homogeneous catalysis, mechanistic studies, DFT calculations*

INTRODUCTION

Efficiency and selectivity constitute decisive factors in the development of sustainable chemical processes, especially regarding industrial large-scale applications. Within this context, the catalytic reduction of carbonyl compounds using molecular hydrogen represents a green and economical method to access valuable alcohols for the production of a large number of fine and bulk chemicals.[1] Over the last few decades, a wide variety of highly productive homogeneous catalysts based on noble metals have been developed for this purpose. However, the selective hydrogenation of carbonyl compounds over other reducible functional groups is still a challenging task. Although significant progress has been made concerning the selective reduction of carbonyl groups in the presence of C=C double bonds,[2] only few examples of catalysts are known which exhibit full selectivity for aldehydes over ketones. In particular, such reactions are important for the production of flavors,[3] fragrances,[3] and pharmaceuticals.[4] Very recently, Dupau and co-workers reported a general and highly efficient method for the chemoselective base-free ruthenium-catalyzed hydrogenation of aldehydes in the presence of ketones. By using the ruthenium complex [Ru(en)(dppe)(OCO*t*Bu)$_2$] (Chart 1), a variety of different ketoaldehydes could by hydrogenated, reaching turnover numbers of up to 40000.[5] Surprisingly, apart from some quite less effective examples,[6] this system remains the only example of a noble-metal-based homogeneous hydrogenation catalyst which allows selective reduction of aldehydes in the presence of ketones.

However, it is a major attractive goal to replace scarce, toxic, and expensive noble metals by environmentally friendly and abundant first-row transition metals.[7,8] Among them, iron appears to be one of the most attractive alternatives.[9] In recent years, significant progress has been achieved in the development of iron-based hydrogenation catalysts.[10] Interestingly, some of these systems proved to be selective for the reduction of aldehydes in the presence of other carbonyl moieties.[11−13] In 2013, Beller and co-workers reported on an Fe(II) tetraphos system (Chart 1) which represents the first example of a homogeneous hydrogenation catalyst exhibiting full chemoselectivity for the reduction of aldehydes.[11] Various substrates including aromatic, aliphatic, and α,β-unsaturated aldehydes could be efficiently converted into the corresponding primary alcohols, while other carbonyl moieties such as ketones and esters were not reduced. Turnover numbers up to 2000 could be achieved at 140 °C and a hydrogen pressure of 40 bar. Even higher TONs were obtained by the group of Milstein using an Fe(II) hydrido carbonyl pincer complex (Chart 1).[12] This complex was found to be highly active also for the hydrogenation of ketones, while its performance in the reduction of aldehydes was only modest.[10g] However, by employing NEt$_3$ as an additive in the reaction, the efficiency of this system could be significantly increased and TONs of up to 4000 were obtained for several substrates under 30 bar of H$_2$ and a reaction temperature of 40 °C. Interestingly, enhanced productivity was also observed in the presence of a large excess of acetophenone, which, however, was found to be unaffected

Received: February 12, 2016
Revised: March 10, 2016
Published: March 11, 2016

DOI: 10.1021/acscatal.6b00436
ACS Catal. 2016, 6, 2664−2672

Chart 1. Well-Defined Catalysts for the Chemoselective Reduction of Aldehydes[5,11−13]

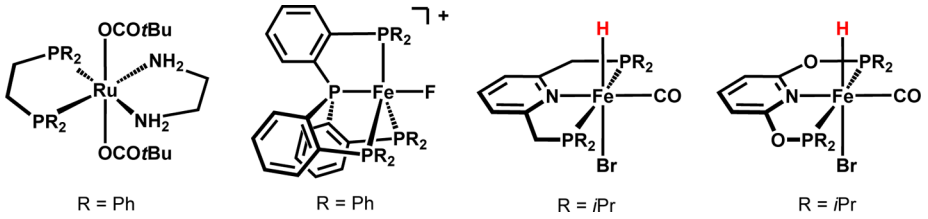

Chart 2. Iron Hydride Complexes Based on the 2,6-Diaminopyridine Scaffold (R = *i*Pr)

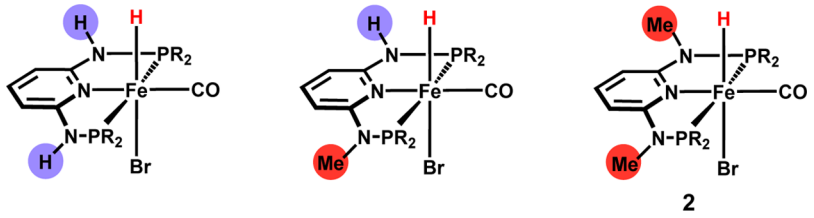

Scheme 1. Synthesis of Complexes 2 and 3 (Mixture of Cis and Trans Isomers)

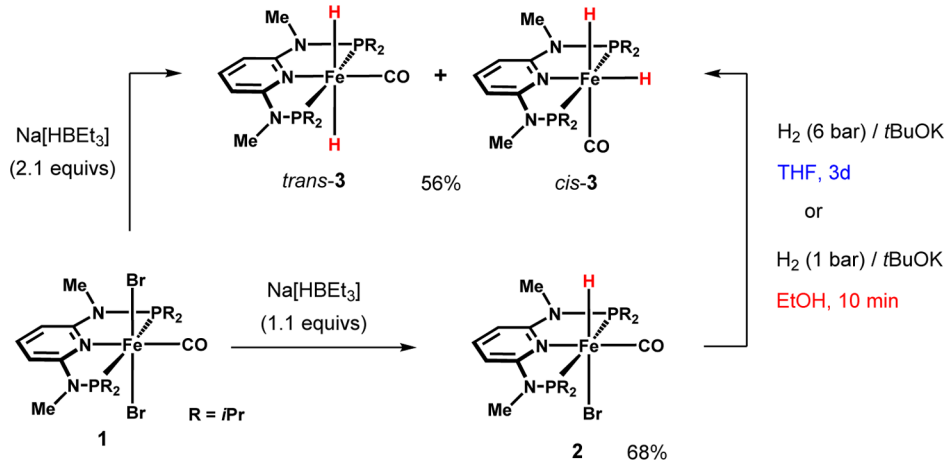

under these conditions. Although briefly mentioned, no further investigations on the chemoselectivity of this catalyst have been provided. More recently, Hu et al. developed a general method for the chemoselective hydrogenation and transfer hydrogenation of aldehydes by using a similar iron(II) pincer complex supported by a 2,6-bis(phosphinito)pyridine ligand (Chart 1).[13] This reaction takes place under very mild conditions (4−8 bar of H_2, room temperature), although high catalyst loadings (5−10 mol %) were required to obtain the primary alcohols in reasonable yields. However, it was remarkable that this reaction did not proceed via a bifunctional mechanism: i.e., involving the pincer ligand.[9d]

Within this context, our group recently reported on the synthesis and reactivity of iron hydride complexes containing PNP pincer ligands based on a 2,6-diaminopyridine scaffold (Chart 2).[14] In these ligands the aromatic pyridine ring and the phosphine moieties are connected via *N*-H or *N*-methyl linkers. The advantage of these ligands is that both substituents on the phosphine and amine sites can be systematically varied in a modular fashion, which has a decisive effect on the outcome of the reactions. Complexes featuring at least one N−H spacer in the ligand backbone efficiently catalyze the hydrogenation of ketones under mild conditions.

On the basis of detailed experimental and computational studies it could be shown that this reaction proceeds via an inner-sphere mechanism in which the catalytically active species is formed by deprotonation of the N−H group. In accordance with the proposed mechanism, no reaction took place when the complex [Fe(PNP^{Me}-*i*Pr)(CO)(H)(Br)] (**2**), which is not capable of this kind of metal−ligand cooperation, was tested. Surprisingly, aldehydes could still be reduced with this complex under the same reaction conditions, thus pointing to an alternative reaction mechanism which allows complete chemoselectivity of aldehydes over ketones. However, these results were just preliminary and the way in which complex **2** is able to promote this reaction remained unclear. In this paper, we provide a detailed catalytic and mechanistic study for the chemoselective reduction of aldehydes using complex **2**, which was found to be the most efficient iron-based hydrogenation catalyst reported to date, displaying unprecedented high turnover numbers surpassing even those of noble-metal catalysts.

RESULTS AND DISCUSSION

The monohydride complex [Fe(PNP^{Me}-*i*Pr)(CO)(H)(Br)] (**2**) was prepared as described previously by the reaction of [Fe(PNP^{Me}-*i*Pr)(CO)$(Br)_2$] (**1**) with Na[$HBEt_3$] (1.1 equiv) in THF (Scheme 1). With this procedure typically two isomers were formed.[14] The major isomer of **2**, with the hydride ligand

DOI: 10.1021/acscatal.6b00436
ACS Catal. 2016, 6, 2664−2672

being trans to the bromide ligand, could be isolated in pure form in 68% isolated yield.

Interestingly, by using 2 equiv of $Na[HBEt_3]$ the corresponding iron(II) dihydride complexes **3** are obtained, which exist of a mixture of cis (major) and trans isomers (minor) in an approximate ratio of 1.0:0.7 (Scheme 1). These new complexes could be isolated in 56% yield and were fully characterized by a combination of elemental analysis and ^1H, $^{13}C\{^1H\}$, and $^{31}P\{^1H\}$ NMR and IR spectroscopy. The $^{31}P\{^1H\}$ NMR spectrum displays two signals at 191.1 and 189.2 ppm for the cis and trans isomers, respectively. In the $^{13}C\{^1H\}$ NMR spectrum two triplets centered at 224.7 and 219.5 ppm were observed for the carbonyl ligands, while only one mutual strong band at 1880 cm^{-1} was found for the CO vibration in the IR spectrum. In the ^1H NMR spectrum, *trans*-**3** exhibits a sharp triplet at −8.76 ppm (J_{PH} = 42.9 Hz) while a broad signal centered at −13.02 ppm is observed for *cis*-**3** due to fast interchange of the two hydride ligands. This could be proved by recording NMR spectra at variable temperatures in THF-d_8 (Figure 1).

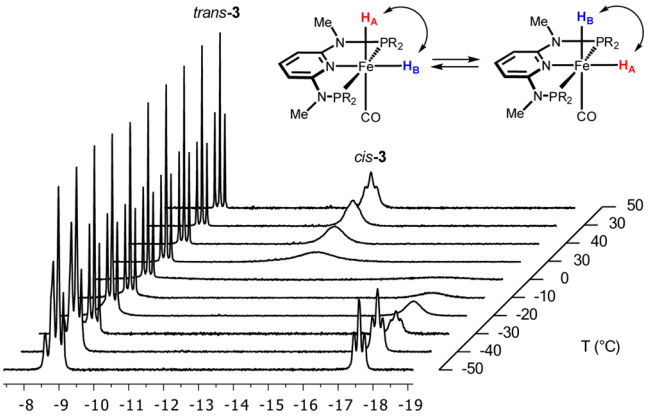

Figure 1. Variable-temperature ^1H NMR spectra of complexes **3** (300 MHz, THF-d_8, hydride region). Complex *cis*-**3** gives rise to signals at −8.82 (H_A) and −17.64 ppm (H_B) at −50 °C. At this temperature the signal of H_A is superimposed with that of the hydrides of *trans*-**3** (−8.76 ppm).

Upon cooling, the broad signal originating from the cis isomer starts to split into two separate triplets centered at −8.82 and −17.64 ppm, respectively, while the evolution of a single triplet resonance was observed at higher temperatures. In addition, all iron hydride complexes described above could be crystallized and their solid-state structures were determined by X-ray diffraction. Structural views of **2** and **3** are depicted in Figures 2 and 3 with selected bond distances given in the captions.

Alternatively, the iron dihydride could also be prepared in situ by the reaction of complex **2** with *t*BuOK (1.1 equiv) under an atmosphere of H_2. Since **2** is not capable of activating dihydrogen in a bifunctional manner, the formation of **3** likely involves intermolecular cleavage of H_2 with support of the iron center and the external base. The rate of hydrogen cleavage strongly depends on the solvent. Immediate formation of **3** was observed in EtOH (1 bar of H_2), while the same reaction carried out in THF required, even under a hydrogen pressure of 5 bar, up to 3 days in order to achieve complete conversion.

Stoichiometric experiments revealed that **3** readily reacts with aldehydes. Again, significant differences were observed, depending on the choice of the solvent. The addition of 1 equiv of benzaldehyde to a solution of the iron dihydride in an aprotic solvent (Scheme 2) resulted in the formation of a new iron hydride species, which was, however, present only in small concentrations. This new compound, exhibiting a characteristic triplet resonance at −23.55 ppm (J_{PH} = 55.5 Hz) in the hydride region of the ^1H spectrum together with a singlet at 164.9 ppm in the $^{31}P\{^1H\}$ NMR spectrum, was identified as the alkoxide complex **4** generated by the insertion of the aldehyde into one of the metal−hydride bonds of **3** (Figure 4). The intensity of this signal did not change over time but grew with an increase in the amount of added substrate. Thus, addition of up to 20 equiv of aldehyde was necessary to observe complete conversion of the iron dihydride. Moreover, no reaction took place when the solution of the in situ generated hydrido alkoxide complex was exposed to dihydrogen (24 h, 6 bar).

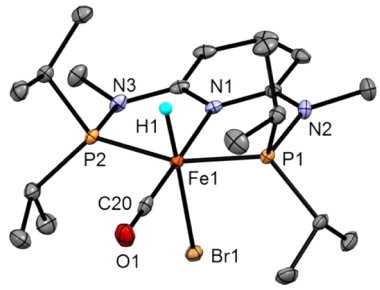

Figure 2. Structural view of [Fe(PNP^{Me}-*i*Pr)(CO)(H)(Br)] (**2**) showing 50% thermal ellipsoids (most H atoms and second independent molecule omitted for clarity). Selected bond lengths (Å) and angles (deg): Fe1−Br1 2.5159(4), Fe1−P1 2.1679(6), Fe1−P2 2.1764(6), Fe1−N1 2.0097(16), Fe1−C20 1.749(2), Fe1−H1 1.46(3); P1−Fe1−P2 161.99(2), N1−Fe1−C20 177.64(9).

In contrast to this, the iron dihydride immediately disappeared after the addition of 1 equiv of benzaldehyde when the reaction was carried out in ethanol (Scheme 3). In this case, two new complexes were observed in the ^1H and $^{31}P\{^1H\}$ NMR spectra. The first complex was again found to be the hydrido alkoxide **4** resulting from substrate insertion, displaying just slightly deviating chemical shifts due to the different solvent. The second complex exhibits a triplet resonance at −26.38 ppm (J_{PH} = 58.9 Hz) in the ^1H spectrum which correlates to a signal at 159.4 ppm in the $^{31}P\{^1H\}$ NMR spectrum and was identified as a cationic species, in which the alkoxide trans to the hydride is replaced by a solvent molecule (**4′**). This complex could be independently synthesized by treatment of **2** with silver salts in ethanol. Purging this mixture with dihydrogen led immediately to the re-formation of the iron dihydride **3**. These findings strongly indicate that the use of a protic solvent is essential for the hydrogenation reaction by labilizing and solvatizing the alkoxo ligand trans to the hydride. In particular, this effect appears to be responsible for the irreversibility of the insertion step by preventing *β*-hydride elimination of the coordinated alkoxide. In the same way, the coordination of dihydrogen to the iron metal center might be facilitated, thus accelerating the rate of H_2 activation. It is worth noting that complex **3** did not react with acetophenone, presumably due to the lower electrophilicity of ketones.

Since the reactivity of a transition-metal hydride is mainly affected by its coligand in the trans position, we therefore expected that only the trans isomer is reactive toward aldehydes and that both isomers are in equilibrium with one another (Scheme 4).[15]

DOI: 10.1021/acscatal.6b00436
ACS Catal. 2016, 6, 2664−2672

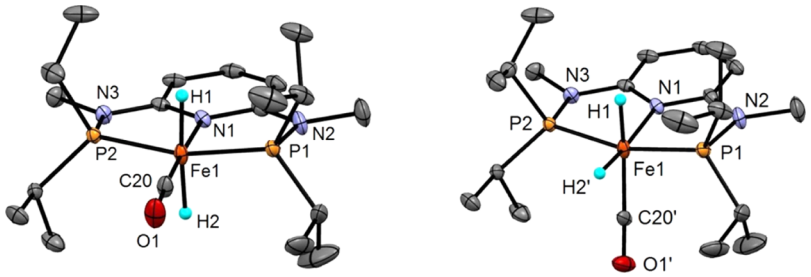

Figure 3. Structural views of (left) *trans*-[Fe(PNP^{Me}-*i*Pr)(H)$_2$(CO)] (*trans*-**3**) and (right) *cis*-[Fe(PNP^{Me}-*i*Pr)(H)$_2$(CO)] (*cis*-**3**) showing 50% thermal ellipsoids (most H atoms omitted for clarity). Selected bond lengths (Å) and angles (deg): Fe1−P1 2.1270(4), Fe1−P2 2.1258(4), Fe1−N1 1.9920(8), Fe1−C20 1.683(3), Fe1−C20′ 1.815(3), Fe1−H1 1.46(2), Fe1−H2 1.46(4), Fe1−H2′ 1.46(2); P1−Fe1−P2 164.09(2), N1−Fe1−C20 177.3(1), N1−Fe1−C20′ 104.7(1).

Scheme 2. Reaction of 3 with Benzaldehyde in C_6D_6

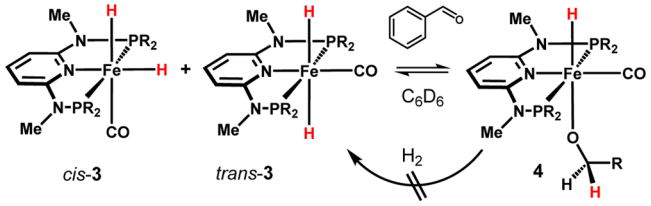

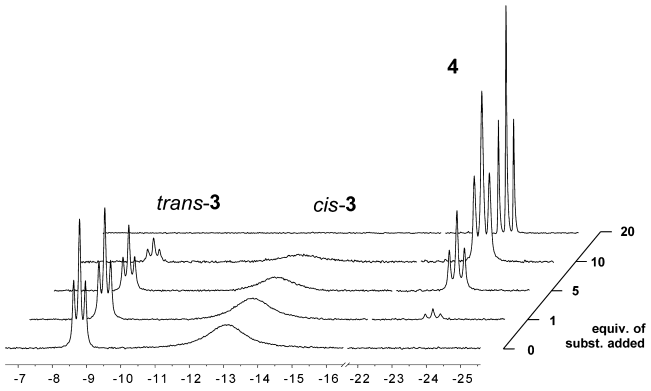

Figure 4. ^{1}H NMR spectra (250 MHz, C_6D_6, hydride region) of **3** in the presence of increasing amounts of benzaldehyde, showing the formation of the corresponding alkoxide complex **4**.

Scheme 4. Reaction of 3 with Benzaldehyde in EtOH[a]

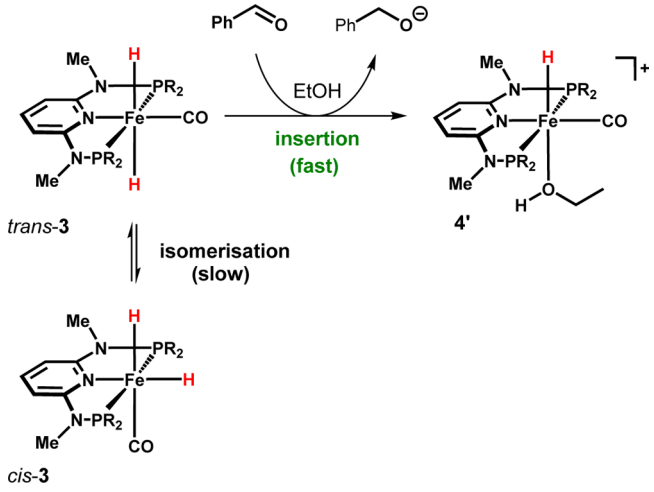

[a]See Figure 5.

The cis/trans isomerization was thought to take place within minutes, since no exchange could be observed on the NMR time scale (^{1}H−^{1}H EXSY). Thus, another experiment was performed by adding only 0.5 equiv of benzaldehyde to a solution of **3** in ethanol and the reaction was continuously

Scheme 3. Reaction of 3 with 1 equiv of Benzaldehyde in EtOH[a]

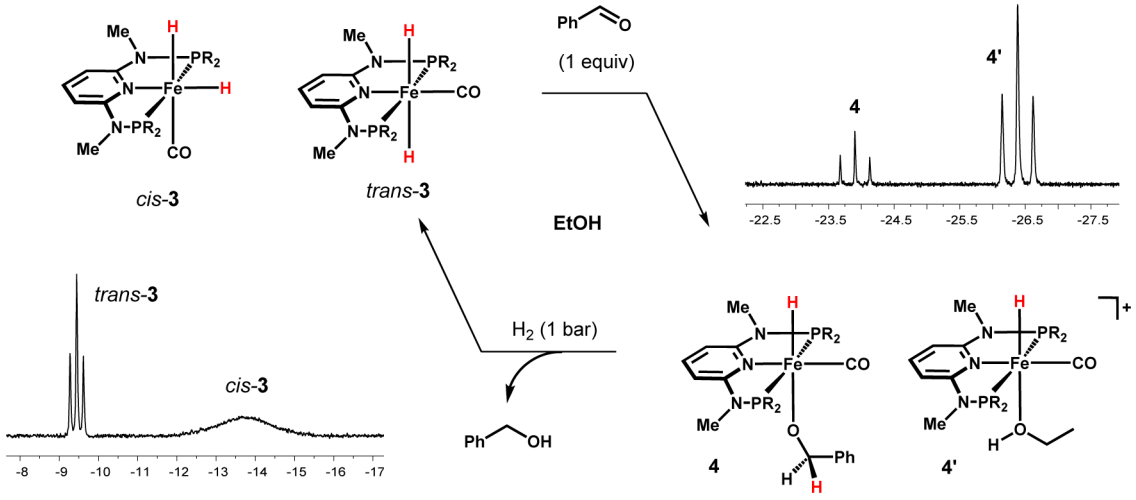

[a]The inset gives the hydride region of the ^{1}H NMR spectra of *cis*- and *trans*-**3** as well as the akoxide and ethanol complexes **4** and **4′**, respectively, at room temperature.

DOI: 10.1021/acscatal.6b00436
ACS Catal. 2016, 6, 2664−2672

monitored by $^{31}P\{^{1}H\}$ NMR spectroscopy. As depicted in Figure 5, the signal of *trans*-**3** immediately disappeared and a new signal was found again for the ethanol complex **4′**, whereas the concentration of *cis*-**3** remained almost unaffected. In this case, the hydrido alkoxide complex was not observed, which might be attributed to the lower substrate concentration in comparison to the previous experiments (Scheme 4 and Figure 4). As expected, we observed recovery of the *trans*-dihydride as a result of the slow isomerization process, which required several minutes to again reach its equilibrium state.

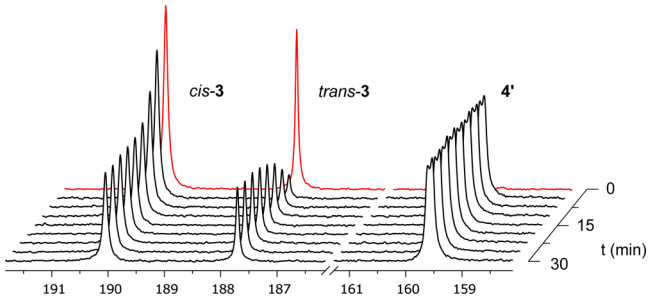

Figure 5. $^{31}P\{^{1}H\}$ NMR spectra (101 MHz, EtOH/C_6D_6) of **3** before (red) and over a period of 30 min after addition of 0.5 equiv of benzaldehyde (black) showing immediate complete conversion of *trans*-**3** into the ethanol complex **4′** followed by recovery of *trans*-**3** via isomerization of *cis*-**3** (due to incomplete proton decoupling the signal of **4′** shows a slight residual coupling to the corresponding hydride ligand).

On the basis of the observations described above, a simplified catalytic cycle is depicted in Scheme 5. The precatalyst **2** readily forms complex *trans*-**3** as a result of heterolytic cleavage of dihydrogen promoted by the iron metal center and the external base. Substrate insertion proceeds presumably through an outer-sphere mechanism in which the nucleophilic dihydride directly attacks the aldehyde's carbonyl group to give the alkoxide intermediate **4**. The compound is labile, and the alkoxide ligand may be replaced either by the solvent (ethanol) to form **4′** or by dihydrogen to form complex **5**, which features an η^2-H_2-bound dihydrogen ligand. Subsequent deprotonation of the coordinated H_2 finally leads to the regeneration of *trans*-**3** and liberation of the product alcohol. Intermediate **5** may be also formed by replacement of the solvent in **4′** by H_2. However, since intermediates **4** and **4′** could be detected by NMR spectroscopy, the question arises as to whether or not these species are indeed part of the catalytic cycle or are merely resting states.

Accordingly, the reaction mechanism was explored in detail by means of DFT calculations.[16] In the model used for the calculations, acetaldehyde was taken as the substrate and *trans*-**3** as the active species. In addition, an explicit ethanol molecule (solvent) was considered, providing a proton shuttle and H-bond stabilization of the intermediates. The free energy profile obtained for the reaction is represented in Scheme 6.[17] The mechanism starts with nucleophilic attack of one hydride ligand of *trans*-**3** to the carbonyl C atom of acetaldehyde (in **A**), with formation of an ethoxide ion that coordinates the metal weakly in a C−H σ complex (**B**). This species is further stabilized by an EtOH···OH bond with the neighboring ethanol molecule. The process is endergonic, with ΔG = 6.3 kcal/mol, and the corresponding barrier ($\Delta G^{\ddagger}$ = 12.0 kcal/mol) indicates a facile process.

The second step of the mechanism corresponds to dissociation of the C−H coordinated ethoxide, yielding a cationic Fe complex with one free coordination position (**C**). The process has a small barrier of 1.1 kcal/mol and is essentially thermoneutral (ΔG = 1.0 kcal/mol). The free coordination position in **C** may be occupied by three different species. One possibility is, naturally, a solvent molecule

Scheme 5. Proposed Simplified Catalytic Cycle for the Chemoselective Hydrogenation of Aldehydes with Dihydrogen To Give Alcohols on the Basis of Experimental Findings

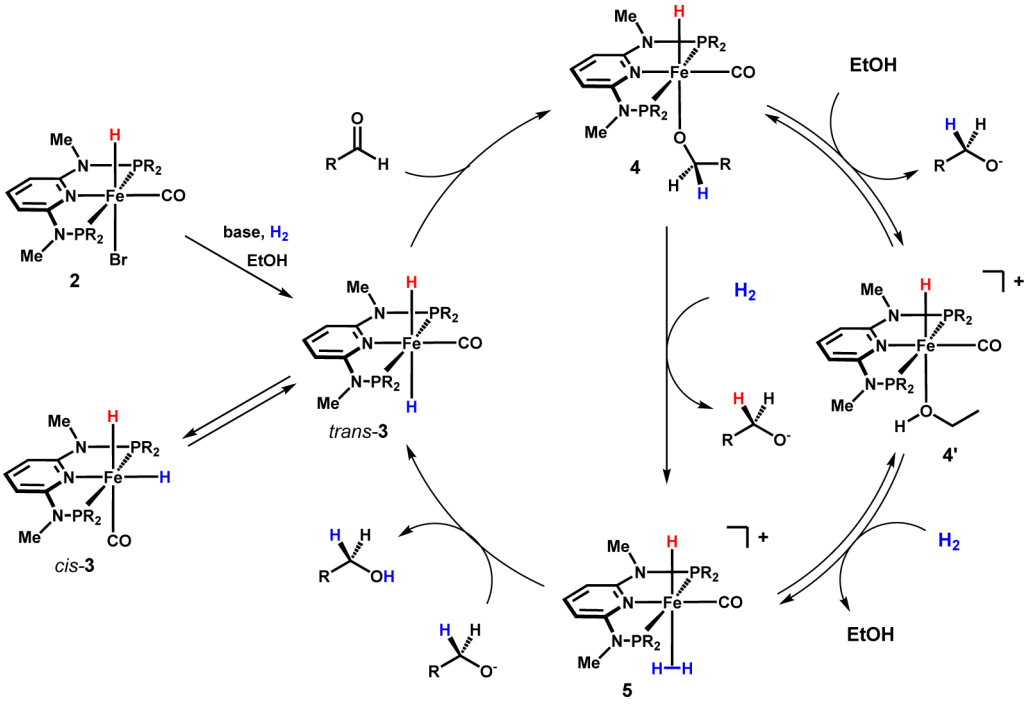

DOI: 10.1021/acscatal.6b00436
ACS Catal. 2016, 6, 2664−2672

Scheme 6. Free Energy Profile Calculated (DFT) for the Hydrogenation of Acetaldehyde by H_2, Catalyzed by *trans*-3[a]

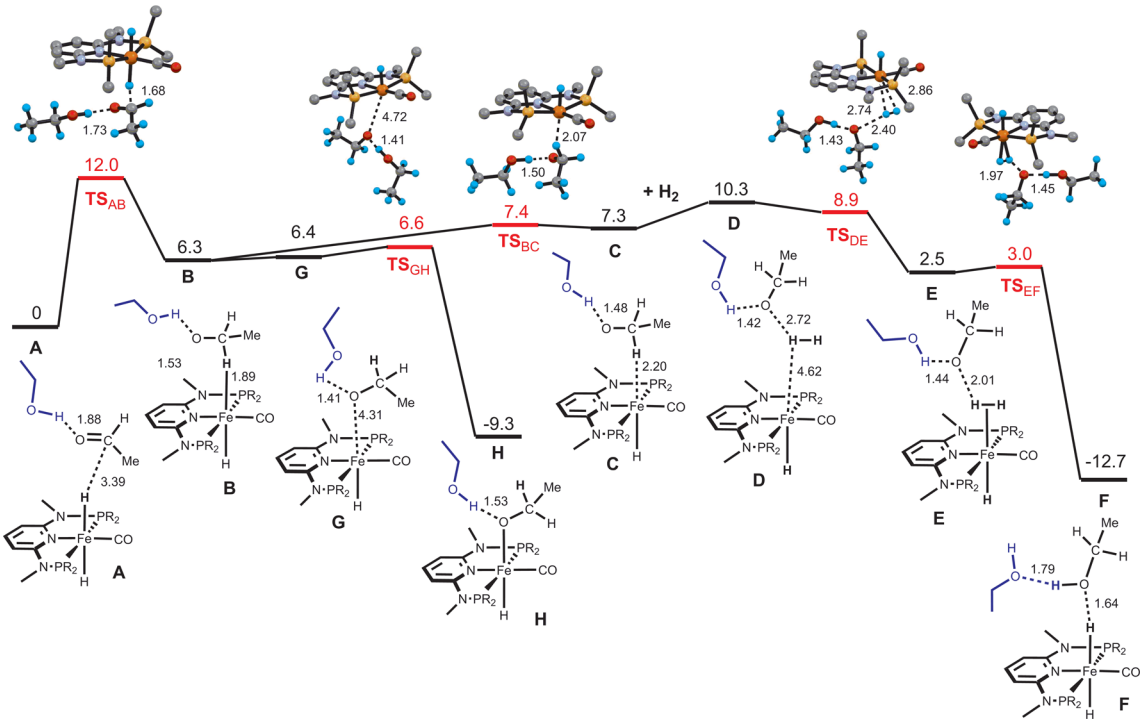

[a]The free energy values (kcal/mol, solvent corrected, EtOH) are referred to the initial reactants (**A**), and relevant distances (Å) are indicated.

Table 1. Hydrogenation of 4-Fluorobenzaldehyde with Catalyst 2[a]

entry	S/C	*P* (bar)	*T* (°C)	base (mol %)	*t* (h)	conversion (%)[b]	TON	TOF (h^{-1})
1	2000	6	room temp	*t*BuOK (1.0)	0.5	>99	2000	4000
2	10000	6	room temp	*t*BuOK (1.0)	24	>99	10000	417
3	10000	30	room temp	*t*BuOK (1.0)	1	>99	10000	10000
4	10000	30	room temp	*t*BuOK (0.5)	1	>99	10000	10000
5	10000	30	room temp	*t*BuOK (0.4)	1	50	5000	5000
6	10000	30	room temp	*t*BuOK (0.3)	1	18	1800	1800
7	10000	30	room temp	*t*BuOK (0.2)	1	<1	0	0
8	20000	30	room temp	*t*BuOK (0.5)	1	62	12300	12300
9	20000	30	room temp	*t*BuOK (1.0)	1	73	14600	14600
10	20000	30	40	*t*BuOK (1.0)	1	93	18600	18600
11	20000	30	room temp	*t*BuOK (2.5)	1	33	6600	6600
12	20000	30	room temp	DBU (1.0)	1	46	9200	9200
13	20000	30	40	DBU (1.0)	1	85	17000	17000
14	20000	30	40	DBU (5.0)	1	91	18200	18200
15	20000	30	40	DBU (1.0)	16	>99	20000	1250
16	20000	60	40	DBU (1.0)	1	>99	20000	20000
17[c]	40000	60	40	DBU (1.0)	16	>99	40000	2500
18[d]	80000	60	40	DBU (1.0)	48	>99	80000	1667

[a]Reaction conditions unless stated otherwise: **2** (0.1−1.0 μmol, 50−500 ppm), 4-fluorobenzaldehyde (2 mmol), base (0.2−5.0 mol %), EtOH (1 mL). [b]Determined by ^{19}F NMR spectroscopy; average of two runs. [c]Reaction conditions 4-fluorobenzaldehyde (4 mmol), EtOH (2 mL). [d]Reaction conditions 4-fluorobenzaldehyde (8 mmol), EtOH (4 mL).

(ethanol) producing complex **4′** as depicted in Schemes 4 and 5. This is a facile process with a barrier of only 2.7 kcal/mol and a free energy balance of ΔG = −2.4 kcal/mol (see Figure S1 in the Supporting Information). Alternatively, there can be O-coordination of the recently formed ethoxide ion, resulting in complex **H** (**4**) and exhibiting a negligible barrier (0.2 kcal/mol), being a considerably exergonic process (ΔG = −15.7 kcal/mol). In fact, the alkoxide complex **H** is 9.3 kcal/mol more stable than the initial reactants, being by far the most stable intermediate along the reaction mechanism and, thus, representing the catalyst resting state. Finally, the free coordination position in **C** can be occupied by one dihydrogen molecule, giving rise to formation of the dihydrogen complex **E**. This process is clearly exergonic (ΔG = −7.8 kcal/mol) and essentially barrierless. The final step corresponds to the breaking of the H−H bond in the dihydrogen complex **E**, with protonation of the nearby ethoxide ion and regeneration of the dihydride species (in **F**). This is a facile process with a barrier of only 0.5 kcal/mol, being largely exergonic (ΔG = −15.2 kcal/mol). Overall, the reaction is exergonic with ΔG =

DOI: 10.1021/acscatal.6b00436
ACS Catal. 2016, 6, 2664−2672

−12.7 kcal/mol, and closing the cycle exchanging one ethanol molecule (the reaction product) with a new acetaldehyde molecule (the substrate), from **F** back to **A**, is slightly endergonic, with a free energy balance of ΔG = 4.1 kcal/mol. The highest barrier of the entire process corresponds to substitution of ethoxide in **H** by one H_2 molecule, in order to allow the reaction to continue. Therefore, the overall barrier for the process is the difference between the free energy values of **H** and TS_{DE}, being ca. 20 kcal/mol, in good agreement with the experimental conditions used for the reaction. It has to be noted that a similar mechanism was proposed recently by Yang, albeit for the reduction of ketones rather than aldehydes.[18]

Since the preliminary catalytic reactions were obtained with high catalyst loadings, more extensive test reactions were performed here in order to investigate the catalytic performance of complex **2**. Initial experiments were conducted in EtOH using 4-fluorobenzaldehyde as substrate (Table 1). In presence of 0.05 mol % of **2** together with 1.0 mol % of *t*BuOK, full conversion to the corresponding primary alcohol was achieved within 30 min at room temperature and a hydrogen pressure of 6 bar. In accordance with our observations on a stoichiometric level, no reaction took place in aprotic solvents such as THF and toluene. A possible transfer-hydrogenation mechanism in EtOH could be excluded, since the reduction of 4-fluorobenzaldehyde was not observed in the absence of dihydrogen.

Decreasing the catalyst loading led to significantly lower reaction rates. Nevertheless, although a much longer reaction time was required, full conversion could still be accomplished at a catalyst to substrate ratio of 1:10000, demonstrating the high efficiency and robustness of this system (Table 1, entry 2). As expected, the catalytic activity increased dramatically by applying higher hydrogen pressures. For example, performing the same reaction at 30 bar reduced the reaction time from 24 h to less than 1 h (entry 3), and even 73% of the primary alcohol was obtained at a catalyst to substrate ratio of 1:20000 (entry 9).

The presence of a strong base appeared mandatory for the reaction to occur. By comparing turnover frequencies after 1 h, we found that a certain amount of *t*BuOK is needed in order to maintain the catalyst in its active state. When the base loading was reduced below 1.0 mol %, the initial reaction rates dropped significantly (Table 1, entries 4−7). On the other hand, larger quantities of *t*BuOK also resulted in lower activity (entry 11). In light of the common sensitivity of aldehydes toward highly basic conditions, this result might be attributed to ongoing side reactions of the substrate, which may potentially cause catalyst deactivation. Therefore, weaker bases were also considered. At a substrate to base ratio of 1:100, amines such as NEt_3 and diisopropylethylamine were not effective, whereas DBU (1,8-diazabicyclo[5.4.0]undec-7-ene) was found to be a suitable cocatalyst. Although the catalytic activity was lower in comparison to that of *t*BuOK at room temperature, similar initial turnover frequencies were observed when the reaction temperature was raised to 40 °C and higher base loadings did not diminish the catalytic performance of complex **2** (entries 12−14). Even when a catalyst to substrate ratio of only 1:20000 was used, 73% of the primary alcohol was formed within 1 h and >99% was formed after the same time when the pressure was increased to 60 bar (entry 16), which corresponds to a turnover frequency of more than 20000 h^{-1}.

Finally, by using this protocol a turnover number of 40000 could be reached within 16 h (Table 1, entry 17) and, most impressive, on application of a long reaction time of 48 h full conversion was still achieved at a catalyst to substrate ratio of 1:80000 (corresponds to 12.5 ppm catalyst loading, entry 18), which is one of the highest turnover numbers reached for a selective aldehyde reduction catalyst to date.[19]

In order to prove the general applicability of **2**, a scope of various substrates has been tested (Table 2). The catalytic experiments were conducted in the presence of 50−100 ppm of catalyst together with 1 mol % of DBU at 40 °C and 30 bar of hydrogen pressure, to ensure quantitative conversion for all substrates in a reasonable reaction time (16 h). The best results could be obtained for heteroaromatic substrates and aromatic aldehydes bearing electron-withdrawing halogen substituents on the phenyl ring, while the reduction of benzaldehyde and derivatives with electron-donating groups such as 4-anisaldehyde and 4-tolylaldehyde was slightly slower. Even sterically demanding as well as aliphatic aldehydes could be reduced quantitatively at low catalyst loadings. If present, C=C double bonds remained unaffected, even in the case of challenging α,β-unsaturated substrates such as cinnamaldehydes or the industrially important citral, emphasizing the high selectivity of this system. It has to be noted that the hydrogenation of cinnamaldehyde did not proceed in the presence of *t*BuOK, revealing the benefits of employing DBU as the base in the reaction. Again, higher turnover numbers could be obtained by

Table 2. Hydrogenation of Aldehydes A1−A14 with Catalysts 2[a]

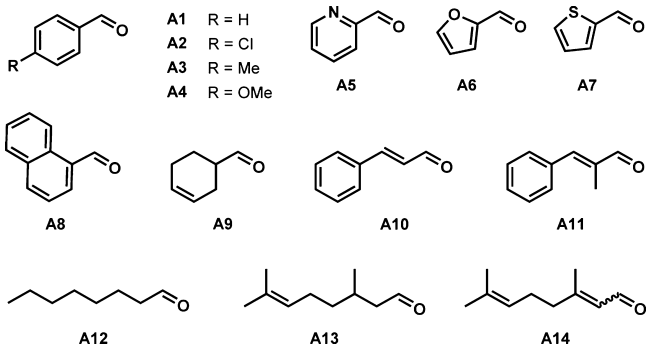

entry	S/C	substrate	conversion (%)[b]	yield (%)[c]
1	20000	**A1**	>99	96
2	20000	**A2**	>99	>99
3	15000	**A3**	>99	>99
4	15000	**A4**	98	98
5	20000	**A5**	>99	97
6	20000	**A6**	>99	>99
7	20000	**A7**	>99	>99
8	10000	**A8**	97	96
9	10000	**A9**	>99	98
10	10000	**A10**	>99	>99
11[d]	20000	**A10**	>99	>99
12	10000	**A11**	>99	>99
13	10000	**A12**	>99	>99
14	10000	**A13**	99	97
15	10000	**A14**	99	99

[a]Reaction conditions unless stated otherwise: catalyst **2** (0.1−0.2 μmol, 50−100 ppm), aldehyde (2 mmol), DBU (20 μmol, 1.0 mol %), EtOH (1 mL), 30 bar of H_2, 40 °C, 16 h. [b]Determined by integration of ^{1}H NMR spectra. [c]Based on integration of ^{1}H spectra using mesitylene as internal standard. [d]Reaction conditions: 60 bar of H_2.

DOI: 10.1021/acscatal.6b00436
ACS Catal. 2016, 6, 2664−2672

Scheme 7. Hydrogenation of 4-Fluorobenzaldehyde in the Presence of Different Cosubstrates Bearing Other Reducible Functionalities

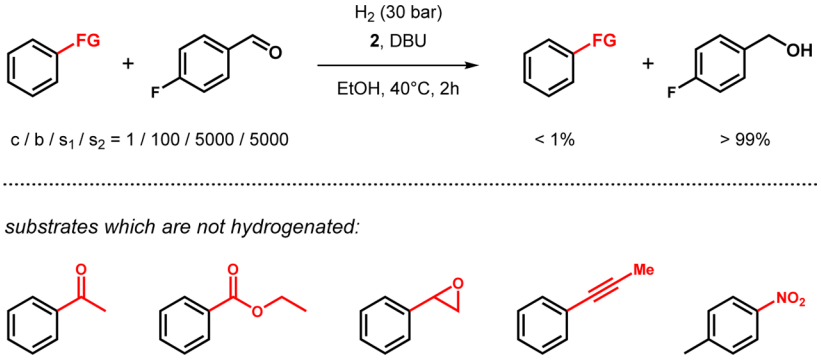

increasing the hydrogen pressure. This was exemplarily shown for cinnamaldehyde, which was quantitatively converted into the corresponding primary alcohol at a catalyst to substrate ratio of 1:20000 at 60 bar of H_2.

Additional tests were carried out in order to investigate the catalyst's selectivity toward other reducible functionalities (Scheme 7). For this purpose, competitive experiments were performed using an equimolar mixture of 4-fluorobenzaldehyde and the respective cosubstrate at a catalyst to substrate ratio of 1:5000 with respect to the aldehyde. Gratifyingly, ketones, esters, epoxides, alkynes, and nitro groups were not hydrogenated and did also not interfere with the reaction.

Since the iron(II) dihydride is supposed to be a key intermediate in the catalytic hydrogenation, we finally conducted a series of test reactions in which the isolated complex **3** was directly used as the catalyst (Table 3). In this case, the addition of an external base was not required. Using cinnamaldehyde as the substrate resulted in full conversion to the corresponding primary alcohol at a catalyst loading of 0.5 mol % within 1 h (30 bar, room temperature), but no reaction took place when the amount of **3** was lowered to 0.1 mol %. This is in accordance with our findings on the influence of the base loading on the catalytic activity, since the overall basicity of the reaction solution now exclusively depends on the amount of the product alkoxide which is initially formed by the insertion of the aldehyde into the metal−hydride bond. However, quantitative formation of cinnamyl alcohol was achieved when the same reaction was carried out in a 2:1 mixture of EtOH and NEt_3.

Table 3. Hydrogenation of Cinnamaldehyde using 3 as Catalyst[a]

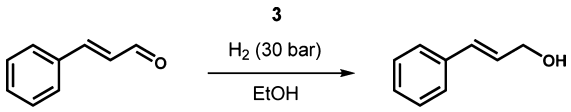

entry	amt of catalyst (mol %)	base	conversion (%)[b]	yield (%)[c]
1	0.5	none	>99	>99
2	0.1	none	0	0
3[d]	0.1	NEt_3	>99	>99

[a]Reaction conditions unless stated otherwise: catalyst **3**, cinnamaldehyde (2.0 mmol), EtOH (1 mL), 30 bar OF H_2, room temperature. [b]Determined by integration of ^1H spectra. [c]Based on integration of ^1H NMR spectra using mesitylene as internal standard. [d]Reaction conditions: EtOH (0.8 mL), NEt_3 (0.4 mL).

CONCLUSION

In sum, an inexpensive and robust homogeneous precatalyst and catalyst using earth-abundant iron, [Fe(PNP^{Me}-*i*Pr)(CO)(H)(Br)] and [Fe(PNP^{Me}-*i*Pr)(H)$_2$(CO)] (mixture of trans and cis isomers), based on the 2,6-diaminiopyridine scaffold where the P*i*Pr$_2$ moieties of the PNP ligand connect to the pyridine ring via NMe spacers, was developed and applied to the hydrogenation of several aldehydes to alcohols in the presence of DBU as base. This methodology proceeds with high chemoselectivity even in the presence of other reducible functional groups such as ketones, esters, alkynes, olefins, and *α,β*-unsaturated double bonds. The yields and chemoselectivities under mild conditions are exceptional in comparison with previous iron catalysts and even noble-metal catalysts. In some cases, full conversion was achieved even at a catalyst to substrate ratio of 1:80000 (12.5 ppm catalyst loading). Accordingly, [Fe(PNP^{Me}-*i*Pr)(CO)(H)(Br)] and [Fe(PNP^{Me}-*i*Pr)(H)$_2$(CO)] are some of the most efficient hydrogenation catalysts for this process to date. On the basis of stoichiometric experimental and computational studies, a mechanism which indeed proceeds via the *trans*-dihydride complex [Fe(PNP^{Me}-*i*Pr)(H)$_2$(CO)] is proposed. Thus, the low catalyst loadings (typically 50 ppm), mild reaction conditions (40 °C, 30 bar of H_2), the broad applicability, and the mild reaction conditions make these catalysts and this procedure interesting for the synthesis of fine and bulk chemicals.[3]

ASSOCIATED CONTENT

Supporting Information

The Supporting Information is available free of charge on the ACS Publications website at DOI: 10.1021/acscatal.6b00436.

Complete crystallographic data, ^1H, $^{13}C\{^1H\}$, and $^{31}P\{^1H\}$ NMR spectra of all complexes, and computational details and coordinates of all optimized species (PDF)

Crystallographic data for **2** and **3** (CCDC entries 1433576 (**2**) and 1433577 (**3**)) (CIF)

AUTHOR INFORMATION

Corresponding Author

*E-mail for K.K.: kkirch@mail.tuwien.ac.at.

Notes

The authors declare no competing financial interest.

DOI: 10.1021/acscatal.6b00436
ACS Catal. 2016, 6, 2664−2672

■ ACKNOWLEDGMENTS

Financial support by the Austrian Science Fund (FWF) is gratefully acknowledged (Project No. P24583−N28). L.F.V. acknowledgesthe Fundação para a Ciência e Tecnologia, Projecto Estratégico- PEst-OE/QUI/UI0100/2013. The X-ray center of the Vienna University of Technology is acknowledged for financial support and for providing access to the single-crystal diffractometer.

■ REFERENCES

(1) (a) *Handbook of Homogeneous Hydrogenation*; de Vries, J. G., Elsevier, C. J., Eds.; Wiley-VCH: Weinheim, Germany, 2007. (b) Dupau, P. In *Organometallics as Catalysts in the Fine Chemical Industry*; Beller, M., Blaser, H. U., Eds.; Springer-Verlag: Berlin, 2012. (c) Johnson, N. B.; Lennon, I. C.; Moran, P. H.; Ramsden, J. A. *Acc. Chem. Res.* **2007**, *40*, 1291−1299. (d) Dub, P. A.; Ikariya, T. *ACS Catal.* **2012**, *2*, 1718−1741.

(2) (a) Noyori, R.; Ohkuma, T. *Pure Appl. Chem.* **1999**, *71*, 1493−1501. (b) Noyori, R.; Ohkuma, T. *Angew. Chem., Int. Ed.* **2001**, *40*, 40−73. (c) Noyori, R. *Angew. Chem., Int. Ed.* **2002**, *41*, 2008−2022. (d) Ohkuma, H.; Ooka, T.; Ikariya, R.; Noyori. *J. Am. Chem. Soc.* **1995**, *117*, 10417−10418.

(3) (a) *Common Fragrance and Flavor Materials*; Surburg, H., Panten, J.; Eds.; Wiley-VCH: Weinheim, Germany, 2006. (b) Saudan, L. A. *Acc. Chem. Res.* **2007**, *40*, 1309−1319.

(4) (a) Smith, A. B.; Barbosa, J.; Wong, W.; Wood, J. L. *J. Am. Chem. Soc.* **1996**, *118*, 8316−8328. (b) Kobayakawa, Y.; Nakada, M. *J. Antibiot.* **2014**, *67*, 483−485.

(5) Bonomo, L.; Kermorvan, L.; Dupau, P. *ChemCatChem* **2015**, *7*, 907−910.

(6) (a) Casey, C. P.; Strotman, N. A.; Beetner, S. E.; Johnson, J. B.; Priebe, D. C.; Guzei, I. A. *Organometallics* **2006**, *25*, 1236−1244. (b) Diab, L.; Smejkal, T.; Geier, J.; Breit, B. *Angew. Chem., Int. Ed.* **2009**, *48*, 8022−8026; *Angew. Chem.* **2009**, *121*, 8166−8170.

(7) *Catalysis Without Precious Metals*; Bullock, R. M., Ed.; Wiley-VCH: Weinheim, Germany, 2010.

(8) Roesler, S.; Obenauf, J.; Kempe, R. *J. Am. Chem. Soc.* **2015**, *137*, 7998−8001.

(9) (a) Morris, R. H. *Chem. Soc. Rev.* **2009**, *38*, 2282−2291. (b) Enthaler, S.; Junge, K.; Beller, M. *Angew. Chem., Int. Ed.* **2008**, *47*, 3317−3321. (c) Gaillard, S.; Renaud, J.-L. *ChemSusChem* **2008**, *1*, 505−509. (d) Bauer, G.; Kirchner, K. A. *Angew. Chem., Int. Ed.* **2011**, *50*, 5798−5800. (e) Bullock, R. M. *Science* **2013**, *342*, 1054−1055. (f) Sues, P. E.; Demmans, Z.; Morris, R. H. *Dalton Trans.* **2014**, *43*, 7650−7667. (g) Bauer, I.; Knölker, H.-J. *Chem. Rev.* **2015**, *115*, 3170−3387.

(10) (a) Bart, S. C.; Lobkovsky, E.; Chirik, P. J. *J. Am. Chem. Soc.* **2004**, *126*, 13794−13807. (b) Bart, S. C.; Hawrelak, E. J.; Lobkovsky, E.; Chirik, P. J. *Organometallics* **2005**, *24*, 5518−5527. (c) Trovitch, R. J.; Lobkovsky, E.; Chirik, P. *Inorg. Chem.* **2006**, *45*, 7252−7260. (d) Casey, C. P.; Guan, H. *J. Am. Chem. Soc.* **2007**, *129*, 5816−5817. (e) Trovitch, R. J.; Lobkovsky, E.; Bill, E.; Chirik, P. J. *Organometallics* **2008**, *27*, 1470−1478. (f) Federsel, C.; Boddien, A.; Jackstell, R.; Jennerjahn, R.; Dyson, P. J.; Scopelliti, R.; Laurenczy, G.; Beller, M. *Angew. Chem., Int. Ed.* **2010**, *49*, 9777−9780. (g) Langer, R.; Leitus, G.; Ben-David, Y.; Milstein, D. *Angew. Chem., Int. Ed.* **2011**, *50*, 2120−2124. (h) Langer, R.; Iron, M. A.; Konstantinovski, L.; Diskin-Posner, Y.; Leitus, G.; Ben-David, Y.; Milstein, D. *Chem. - Eur. J.* **2012**, *18*, 7196−7209. (i) Yu, R. P.; Darmon, J. M.; Hoyt, J. M.; Margulieux, G. W.; Turner, Z. R.; Chirik, P. J. *ACS Catal.* **2012**, *2*, 1760−1764. (j) Ziebart, C.; Federsel, C.; Anbarasan, P.; Jackstell, R.; Baumann, W.; Spannenberg, A.; Beller, M. *J. Am. Chem. Soc.* **2012**, *134*, 20701−20704. (k) Fleischer, S.; Zhou, S.; Junge, K.; Beller, M. *Angew. Chem., Int. Ed.* **2013**, *52*, 5120−5124. (l) Srimani, D.; Diskin-Posner, Y.; Ben-David, Y.; Milstein, D. *Angew. Chem., Int. Ed.* **2013**, *52*, 14131−14134. (m) Wienhofer, G.; Baseda-Kruger, M.; Ziebart, C.; Westerhaus, F. A.; Baumann, W.; Jackstell, R.; Junge, K.; Beller, M. *Chem. Commun.* **2013**, *49*, 9089−9091. (n) Bornschein, C.; Werkmeister, S.; Wendt, B.; Jiao, H.; Alberico, E.; Baumann, W.; Junge, H.; Junge, K.; Beller, M. *Nat. Commun.* **2014**, *5*, 4111. (o) Chakraborty, S.; Dai, H.; Bhattacharya, P.; Fairweather, N. T.; Gibson, M. S.; Krause, J. A.; Guan, H. *J. Am. Chem. Soc.* **2014**, *136*, 7869−7872. (p) Chakraborty, S.; Lagaditis, P. O.; Förster, M.; Bielinski, E. A.; Hazari, N.; Holthausen, M. C.; Jones, W. D.; Schneider, S. *ACS Catal.* **2014**, *4*, 3994−4003. (q) Lagaditis, P. O.; Sues, P. E.; Sonnenberg, J. F.; Wan, K. Y.; Lough, A. J.; Morris, R. H. *J. Am. Chem. Soc.* **2014**, *136*, 1367−1380. (r) Werkmeister, S.; Junge, K.; Wendt, B.; Alberico, E.; Jiao, H.; Baumann, W.; Junge, H.; Gallou, F.; Beller, M. *Angew. Chem., Int. Ed.* **2014**, *53*, 8722−8726. (s) Bertini, F.; Mellone, I.; Ienco, A.; Peruzzini, M.; Gonsalvi, L. *ACS Catal.* **2015**, *5*, 1254−1265. (t) Rivada-Wheelaghan, O.; Dauth, A.; Leitus, G.; Diskin-Posner, Y.; Milstein, D. *Inorg. Chem.* **2015**, *54*, 4526−4538. (u) Zhang, Y.; MacIntosh, A. D.; Wong, J. L.; Bielinski, E. A.; Williard, P. G.; Mercado, B. Q.; Hazari, N.; Bernskoetter, W. H. *Chem. Sci.* **2015**, *6*, 4291−4299.

(11) Wienhofer, G.; Westerhaus, F. A.; Junge, K.; Ludwig, R.; Beller, M. *Chem. - Eur. J.* **2013**, *19*, 7701−7707.

(12) Zell, T.; Ben-David, Y.; Milstein, D. *Catal. Sci. Technol.* **2015**, *5*, 822−826.

(13) Mazza, S.; Scopelliti, R.; Hu, X. *Organometallics* **2015**, *34*, 1538−1545.

(14) Gorgas, N.; Stöger, B.; Veiros, L. F.; Pittenauer, E.; Allmaier, G.; Kirchner, K. *Organometallics* **2014**, *33*, 6905−9614.

(15) Eisenstein, O.; Crabtree, R. H. *New J. Chem.* **2013**, *37*, 21−27.

(16) Parr, R. G.; Yang, W. *Density Functional Theory of Atoms and Molecules*; Oxford University Press: New York, 1989.

(17) Intermediate **D** is 1.4 kcal/mol less stable than $\mathbf{TS_{DE}}$. This feature is the result of single-point energy calculations in species with similar stabilities. In fact, at the theory level used in the geometry optimizations, **D** is 4.2 kcal/mol below $\mathbf{TS_{DE}}$.

(18) Yang, X. *Inorg. Chem.* **2011**, *50*, 12836−12843.

(19) Strohmeier, W.; Weigelt, L. *J. Organomet. Chem.* **1978**, *145*, 189−194.

DOI: 10.1021/acscatal.6b00436
ACS Catal. 2016, 6, 2664−2672